Available online at www.sciencedirect.com

jmr&t Journal of Materials Research and Technology

www.jmrt.com.br

Original Article

Effect of laser irradiation on micro-hardness, compactness and Raman spectrum of glassy $Se_{76}Te_{20}Sn_2Cd_2$ alloy

Amit Kumar[a], *Mousa M.A. Imran*[b], *Arvind Sharma*[a], *Neeraj Mehta*[a,*]

[a] *Department of Physics, Institute of Science, Banaras Hindu University, Varanasi 221005, India*

[b] *Materials Science Lab, Department of Physics, Faculty of Science, Al-Balqa Applied University, Al-Salt 19117, Jordan*

ARTICLE INFO

Article history:
Received 24 March 2016
Accepted 4 April 2017
Available online 9 August 2017

Keywords:
Chalcogenide glasses
Laser
Micro-hardness
Raman spectroscopy

ABSTRACT

In present novel work, we have synthesized a novel quaternary $Se_{76}Te_{20}Sn_2Cd_2$ glass in bulk form. Four laser light sources from UV-Vis-IR region have been used to investigate the laser-induced effects on the micro-hardness to check the candidature of this material for possible application in fiber optics. The micro-hardness of the quaternary $Se_{76}Te_{20}Sn_2Cd_2$ glass is increased appreciably after laser exposure. This result has been analyzed in terms of compactness. The enhancement in both micro-hardness and compactness is also explained by Raman spectroscopy.

1. Introduction

Chalcogenide glasses are well-known for their desirable optical properties such as transmission in the infrared, high refractive index and high nonlinearity. Such properties have enabled many chalcogenide-based applications to be developed in diverse fields including photonics, medicine, environmental sensing and security [1–6]. Conventional methods for depositing these materials such as vacuum coating (thermal evaporation, chemical vapor deposition or sputtering) or pulse laser deposition [7] have been used extensively.

The chalcogenide glasses share two common properties that have a profound impact on their interaction with light; their electronic structure and their phonon vibrations [7]. Electronically, the chalcogenide glasses behave as semiconductors. They possess a bandgap, and consequently they are transparent to a certain range of wavelengths of light. The disorder of the glassy network in these materials creates localized electronic states that extend into the forbidden bandgap. These states have a significant effect on the electrical and optical properties of the chalcogenide glasses. The transparent window extends far into the infrared because the infrared side of the transparent region is determined by the phonon energy of the material. The presence of large, heavy atoms shifts the phonons to lower energy and therefore longer wavelengths. The low phonon energy makes the chalcogenide glasses attractive as infrared optical materials [7].

* *Corresponding author.*
E-mail: dr_neeraj_mehta@yahoo.co.in (N. Mehta).

https://doi.org/10.1016/j.jmrt.2017.04.008

Laser irradiation to glass has been regarded as a process for structural modification and/or crystallization in glass. Various workers have used laser as a tool for tailoring of different physical properties of chalcogenide glasses. Khan et al. studied laser-induced amorphization and crystallization on $Se_{80}Te_{20-x}Pb_x$ thin films [8]. Bahishti et al. investigated the Effect of laser irradiation on thermal and optical properties of selenium–tellurium alloy [9]. Lorinczi et al. reported the structural details of the Ag-As_2S_3 interface obtained by vacuum thermal evaporation followed by green laser irradiation [10]. Al-Ghamdi et al. studied the laser irradiation effects on optical constants in thin films of $Ga_{15}Se_{85-x}In_x$ chalcogenide system [11,12]. Naik et al. performed FTIR and XPS measurements to see the laser-induced alterations in the optical properties of $Sb_{10}S_{40}Se_{50}$ chalcogenide thin films [13]. Bahishti et al. observed the Laser Irradiation Effect on the Optical Band Gap of $Se_{96-x}Te_4Hg_x$ thin films [14]. Uddin et al. reported the laser irradiation effect on the optical properties of a-$Se_{88}Te_{12-x}Al_x$ thin films [15].

In above literature survey, the different groups have observed a common feature that the laser irradiation produces defects in the chalcogenide glasses [16]. The presence of defects and irradiation-induced disorder significantly affects the characteristic features of these materials. The investigation of various properties with laser irradiation is also helpful for understanding of the mechanism of degradation in these materials. This motivated us to start work in this significant and recent on-going research activity. In present work, we have synthesized a novel $Se_{76}Te_{20}Sn_2Cd_2$ multicomponent glass. The investigations on the micro-hardness of chalcogenide glasses are of straight practical importance since these materials have various potential applications in infrared fiber optics. Keeping in mind this fact, we have planned the micro-hardness measurements in as-prepared sample and laser-exposed samples of this novel glass. Generally, the composition of the glassy alloy is changed for tailoring of properties. We have used a new trend in which lasers of different wavelengths have been used instead of changing the composition. For this purpose, cw-lasers of four different wavelengths (405 nm, 532 nm, 690 nm and 785 nm) have been used.

2. Theoretical basis

Hardness is a significant mechanical property of materials that is defined as the resistance of a solid object to permanent deformation under pressure. The prediction of hardness has attracted much interest [17,18] since it enables a tailoring of material science to capitulate enhanced mechanical properties. For instance, the hardness of glass is a crucial issue in the development of scratch-resistant glass covers for personal electronic devices.

The Vickers hardness test method is one of the most frequent and consistent methods for hardness measurements. It provides helpful information concerning the mechanical behavior of brittle solids [19]. Moreover, the indentation microhardness is important for understanding the mechanisms of deformation and fracture of materials [20]. Studies on the indentation fracture in brittle materials have also shown that

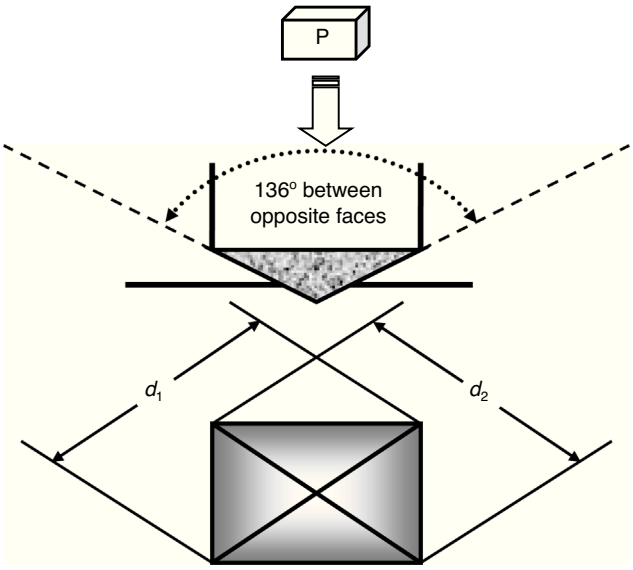

Fig. 1 – Geometry of diamond indenter used as a probe of micro-hardness.

indentation testing is a straightforward technique for characterizing the fracture behavior of glass and ceramics [21]. The indentation is generally carried out using sharp indenters such as a cone or pyramid, because of the geometrical similarity of the residual impressions. The contact pressure with such geometry is independent of indent size and thus affords a convenient measure of hardness [19]. The Vickers hardness test method consists of indenting the test material with a diamond indenter, in the form of a right pyramid with a square base and an angle of 136° between opposite faces subjected to a load (≤100 kgf). The schematic diagram for understanding the geometry of indenter is shown in Fig. 1.

3. Experimental

Bulk sample of quaternary $Se_{76}Te_{20}Sn_2Cd_2$ alloy in glassy form was prepared by recognized quenching technique. The accurate proportions of high purity 5 N (99.999%) elements were weighed in accordance with their atomic percentages. An electronic balance having least count 10^{-4} g was employed for this purpose. The materials were then sealed in evacuated quartz tubes. A high Vacuum pumping system (Hind Hivac, Model: VS65D) with facility of a liquid nitrogen trap was used to achieve suitable vacuum (~10^{-6} Torr). The tube was tucked with a ceramic rod and was heated inside a muffle furnace at an appropriate temperature. During heating, the tube was frequently rocked by rotating the ceramic rod. This was done to make the melt homogeneous. After rocking for about 12 h, the obtained melts were cooled rapidly by removing the tube from the furnace and dropping to ice-cooled water swiftly. The ingots of the sample were then taken out by breaking the quartz tube. The glassy nature of the present glass was confirmed by using XRD and SEM techniques. The SEM photographs and XRD pattern of as-prepared sample of $Se_{76}Te_{20}Sn_2Cd_2$ are shown in Fig. 2. On alert inspection of SEM image, the existence of homogeneous clusters of hierarchical

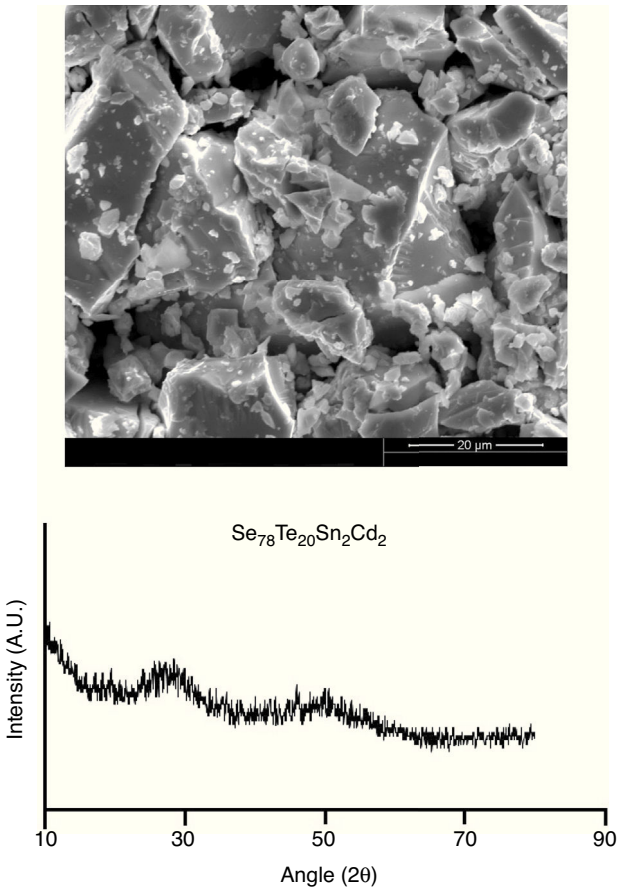

Fig. 2 – SEM image and XRD pattern of glassy $Se_{76}Te_{20}Sn_2Cd_2$ alloy.

surface morphology can be viewed. Fig. 2 also shows the XRD pattern in lower panel of same sample. The absence of any sharp peak also confirms the non-crystalline structure of present sample.

Disk shaped samples (pellets) of identical geometry (diameter ~6 mm and thicknesses ~0.5 mm) were used for micro-indentation testing. Micro-indentation measurements were performed on the specimen using an automated digital Vickers micro-hardness tester (Vaiseshika Electron Devices, Model: DHV-1000). The four pellets are irradiated uniformly using four pulsed lasers of different wavelengths (405 nm, 532 nm, 690 nm and 785 nm) in UV, visible and IR region at fixed intensity (~50 mW) and exposure time (~3 min). The experimental photograph of irradiation of a sample by green diode laser in laboratory is shown in Fig. 3.

4. Results and discussion

Traditional hardness property is measured using a static machine and involves the measurement of the diagonal of the impression after unloading. The Vickers hardness number (VHN)H_v is obtained as the ratio of the applied load (P) to the superficial area of the impression, in kg mm^{-2}. The Vickers indenter is a square based diamond pyramid with included

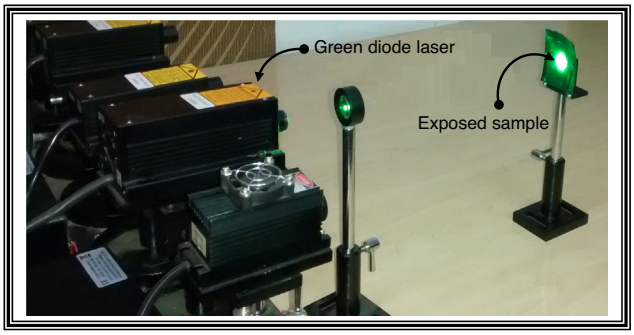

Fig. 3 – Experimental demonstration of illumination of sample of glassy $Se_{76}Te_{20}Sn_2Cd_2$ alloy by green diode laser having wavelength 532 nm.

angle between opposite faces of 136°. The perfect impression is square and has a superficial area of $d^2/2 \sin 68°$.

The formula for calculation of VHN is as follows:

$$H_v = \frac{2P\sin(\theta/2)}{d^2} = \frac{1854.4P}{d^2} \quad (1)$$

Here H_v is Vickers hardness number, P is load in kgf and d is the average diagonal of the impression in mm and θ is the included angle between the faces of the square pyramid ($\theta = 136°$ for a Vickers indenter). The diagonals of the resulting indentations were measured on all specimens directly by using a micrometer eyepiece that was calibrated using a ERMA disk at each magnification.

Fig. 4 shows typical photographs of Vickers indented marks obtained from optical microscope for virgin and exposed samples of quaternary $Se_{76}Te_{20}Sn_2Cd_2$ alloy at 100 g load. In the present study, the hardness behavior due to load was investigated by instrumented indentation with 100 g load examined optically and computer operator software. Each measurement was carried out at least ten times and the mean value of the hardness number was determined at room temperature. The values of micro-hardness H_v for as-prepared and laser-exposed samples of glassy $Se_{76}Te_{20}Sn_2Cd_2$ alloy are given in Table 1 (here we have labeled 0 nm wavelength for the unexposed sample). From this table, it is clear that the value of H_v is increased after laser exposure. The maximum increment in micro-hardness is observed in case of red laser of 690 nm.

Since there is a need of critical number of constraints for a material to display mechanical resistance, therefore the hardness of material is governed by the number of network constraints at room temperature. One of the significant constraints which play crucial role in deciding the hardness of

Table 1 – Values of W_m for unexposed and laser-exposed samples of glassy $Se_{76}Te_{20}Sn_2Cd_2$ alloy.

Wavelength (nm)	H_v (kgf/mm^2)	δ
0	49.4	−0.263
405	51.5	−0.202
532	61.6	−0.122
690	68.7	−0.103
785	56.8	−0.140

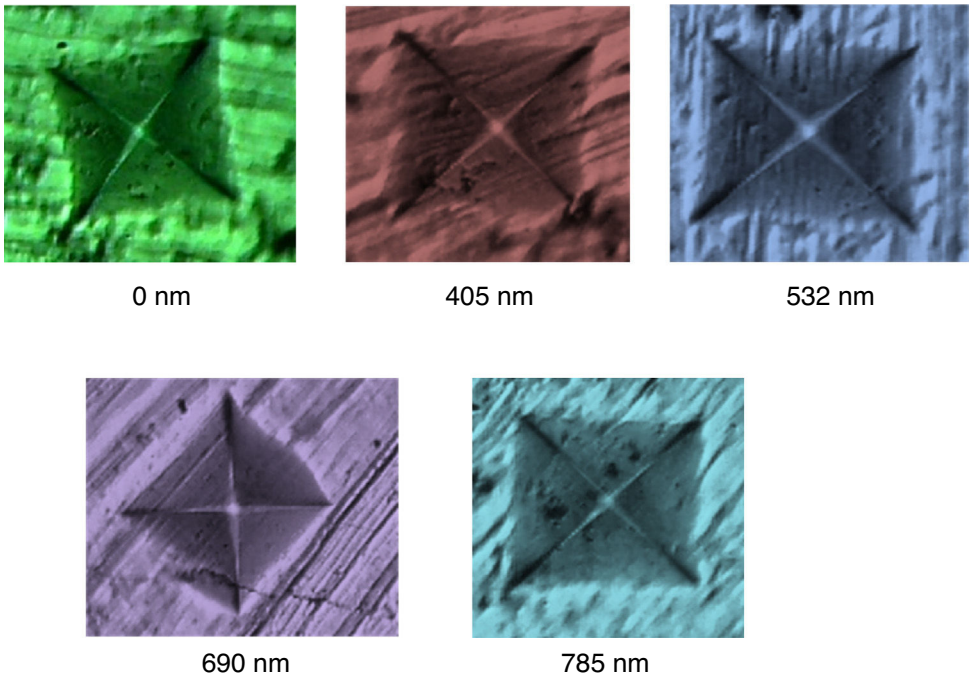

Fig. 4 – Impression of the Vickers indentation on as-prepared and laser-exposed samples of glassy $Se_{76}Te_{20}Sn_2Cd_2$ alloy.

the solid is its compactness. It is associated with the free volume and the flexibility of the network. The compactness can assume negative values, which correspond to larger free volumes and flexibilities. The compactness of the structure of the glasses is determined from the experimentally measured value of density ρ of the glasses.

The compactness (δ) was calculated by the formula [22,23]:

$$\delta = \rho \left[\frac{\sum_i x_i A_i/\rho_i - \sum_i x_i A_i/\rho}{\sum_i x_i A_i} \right] \quad (2)$$

Here x_i, A_i and ρ_i are the respective atomic fraction, the atomic weight and the atomic density of the ith element of the glass and ρ is the measured density of the glass. The compactness is a measure of the normalized change of the mean atomic volume due to chemical interactions of the elements forming the network of a given solid [24]. Consequently, it is more sensitive to changes in the structure of the glass network as compared to the mean atomic volume. The calculated values of δ for as-prepared and laser-exposed samples of glassy $Se_{76}Te_{20}Sn_2Cd_2$ alloy are also listed in Table 1. From this table, it is clear that the value of δ is also increased after laser exposure. The maximum increase in compactness is also observed in case of red laser of 690 nm. Thus, one can expect that the micro-hardness of the samples is increased with increase in its compactness. To verify this fact, we have plotted a graph between VHN and compactness in Fig. 5. From this figure, one can see that the plot of H_v versus δ is almost a straight line having adequate co-relation coefficient.

Chalcogenide glasses are soft semiconductors due to the two-fold coordinated chalcogen atoms. Consequently, they behave as a flexible electron-lattice coupling system when they are subject to exhibit electro-atomic responses [3]. Therefore, the enhancement in Vickers hardness of present sample after laser exposure can also be understood as a consequence of a fact that the anharmonic phonons are very sensitive to the increased temperature for the chalcogenide glasses [3,25]. However, it will be a subject of a separate work in future.

As a part of the efforts to understand the structure of chalcogenide glasses network as well the structural change which can occur after illumination, Raman scattering continues to provide useful insights into the local structures of the vitreous state. The shift of the main Raman peaks can be attributed to the changed chemical environment. Therefore, we have used Raman spectroscopy to determine as far as possible the structural change which can occur in this glass after laser exposure. Fig. 6 presents Raman spectra for as-prepared and laser-exposed samples of glassy $Se_{76}Te_{20}Sn_2Cd_2$ alloy in wavenumber range 100–900 cm^{-1}. It is interesting to note that we have found two significant peaks around 198 cm^{-1} and 275 cm^{-1} [see Fig. 7(a) and (b)].

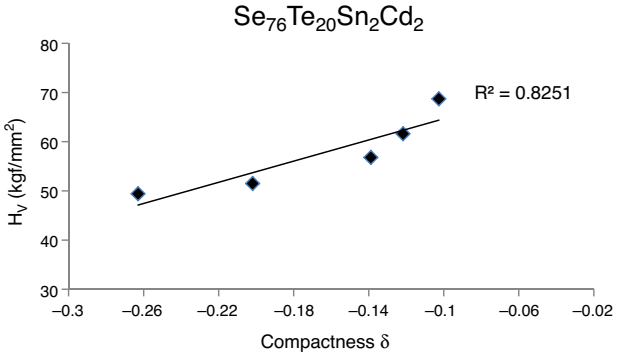

Fig. 5 – Plot of micro-hardness versus compactness for glassy $Se_{76}Te_{20}Sn_2Cd_2$ alloy.

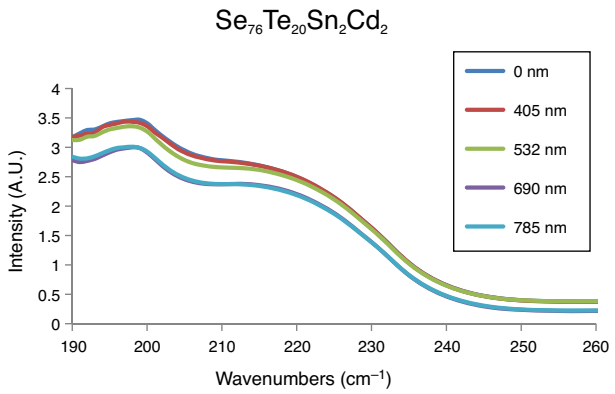

Fig. 6 – Raman spectra of as-prepared and laser-exposed samples of glassy $Se_{76}Te_{20}Sn_2Cd_2$ alloy.

The Raman band corresponding to 275 cm^{-1} is generally assigned to the characteristic vibrational mode of the Selenium atoms in amorphous phase that consists of Se chains and rings as well as other mixed units. The Raman band corresponding to 198 cm^{-1} is assigned to the bending modes of Se units. The vibration band at 198 cm^{-1} is of special interest. Its intensity decreases for samples exposed by diode lasers; irrespective of wavelength. This new feature can be attributed to the enhancement in $Sn(Se_{1/2})_4$ tetrahedral units [26]. However, we cannot suggest more rigorous and detailed structure model of the present multi-component glass because of the absence of more detailed experimental data for quaternary glasses. Future experiments may reveal the exact knowledge of molecular structure in such complex glassy networks.

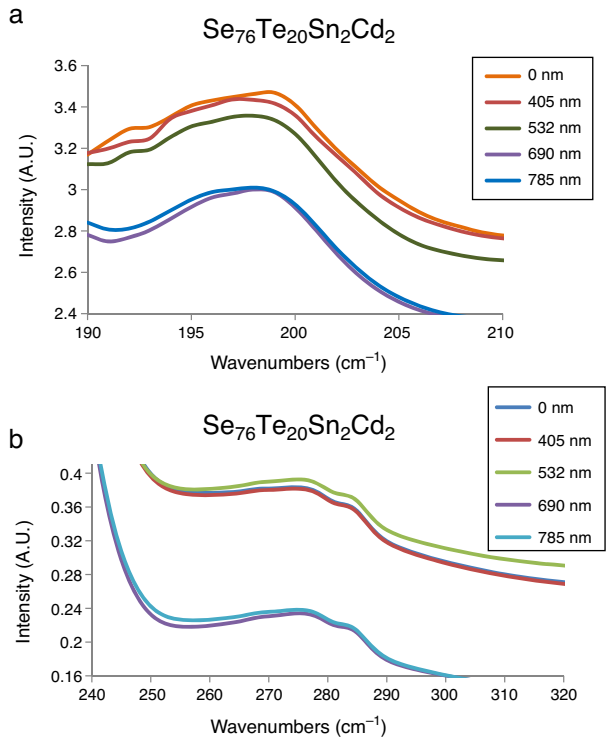

Fig. 7 – Observation of Raman peaks around (a) 198 cm^{-1} and (b) 275 cm^{-1}.

The careful inspection of the afore said Raman peaks shown in Fig. 7(a) confirm that these peaks slightly move toward smaller wavenumber for laser exposed samples. A possible reason of the peak displacement can be expressed in terms of consequences occurred due to local heating of glassy network under laser exposure. When we expose the sample by the laser, the sample is warmed up a little bit locally. This local heating causes stress in the amorphous network inducing increase of the spring force and thus the vibrational modes shifts to smaller wavenumbers. This is probably the reason of increase of compactness and hence the increase in micro-hardness after laser exposure. Thus, the Raman analysis supports the observed increment in the values of H_v and δ after laser exposure.

5. Conclusions

Hardness and density measurement as well as Raman analysis has been done in samples of as-prepared novel multi-component $Se_{76}Te_{20}Sn_2Cd_2$ glass and its laser-exposed samples. The hardness of the exposed samples is increased after illumination by four laser light sources having wavelengths in UV-Vis-IR region. The enhancement of micro-hardness is increased in terms of raise in the compactness of the exposed samples. The VHN is increased almost linearly with compactness. Analysis of Raman spectra shows the evidence of increase in the spring force owing to stress generation in the amorphous network after laser exposure. This provides the basis for the observed enhancement in micro-hardness H_v and compactness δ.

Conflicts of interest

The authors declare no conflicts of interest.

Acknowledgement

NM and AK are thankful to the Department of Science and Technology (DST), Delhi, India for providing financial assistance under Fast Track Young Scientists Scheme [Scheme No. SR/FTP/PS-054/2010].

REFERENCES

[1] Ohta T. Phase-change optical memory promotes the DVD optical disk. J Optoelectron Adv Mater 2001;3:609–26.
[2] Andriesh AM, Lovu MS, Shutov SD. Chalcogenide non-crystalline semiconductors in optoelectronics. J Optoelectron Adv Mater 2002;4:631–47.
[3] Popescu M. Disordered chalcogenide optoelectronic materials: phenomena and applications. J Optoelectron Adv Mater 2005;7:2189–210.
[4] Hamann HF, O'Boyle M, Martin YC, Rooks M, Wickramasinghe HK. Ultra-high-density phase-change storage and memory. Nat Mater 2006;5:383–7.
[5] Wuttig M, Yamada N. Phase-change materials for rewritable data storage. Nat Mater 2007;6:824–32.

[6] Lencer D, Salinga M, Grabowski B, Hickel T, Neugebauer J, Wuttig M. A map for phase change materials. Nat Mater 2008;7:972–7.
[7] Mehta N. Application of chalcogenide glasses in electronics and optoelectronics. J Sci Ind Res 2006;65:777–86.
[8] Khan SA, Zulfequar M, Husain M. Laser-induced amorphization and crystallization on $Se_{80}Te_{20-x}Pb_x$ thin films. Vacuum 2004;72:291–6.
[9] Bahishti AA, Khan MAM, Patel BS, Al-Hazmi FS, Zulfequar M. Effects of laser irradiation on thermal and optical properties of selenium-tellurium alloy. J Non-Cryst Solids 2009;355:2314–7.
[10] Lorinczi A, Velea A, Matei E, Simandan I-D, Popescu M. Structural details of the Ag-As_2S_3 interface obtained by vacuum thermal evaporation followed by green laser irradiation. Chalcogenide Lett 2010;7: 609–12.
[11] Al-Ghamdi AA, Khan SA, Al-Heniti S, Al-Agel FA, Zulfequar M. Annealing and laser irradiation effects on optical constants of $Ga_{15}Se_{85}$and $Ga_{15}Se_{83}In_2$ chalcogenide thin films. Curr Appl Phys 2010;11:315–20.
[12] Al-Ghamdi AA, Khan SA, Al-Heniti S, Al-Agel FA, Al-Harbi T, Zulfequar M. Effects of laser irradiation on optical properties of amorphous and annealed $Ga_{15}Se_{81}In_4$ and $Ga_{15}Se_{79}In_6$ chalcogenide thin films. J Alloys Compd 2010;505: 229–34.
[13] Naik R, Jena S, Ganesan R, Sahoo NK. Laser-induced optical properties change in $Sb_{10}S_{40}Se_{50}$ chalcogenide thin films: an investigation through FTIR and XPS measurements. Phys Solid Stat b 2014;251:661–8.
[14] Bahishti AA, Uddin I, Zulfequar M, Alharbi T. Laser irradiation effect on the optical band gap of $Se_{96-x}Te_4Hg_x$ thin films. J Mod Mater 2016;1:17–23.
[15] Uddin I, Howari H, Ansari GA. Laser irradiation effect on the optical properties of a-$Se_{88}Te_{12-x}Al_x$ thin films. Chalcogen Lett 2016;13:117–25.
[16] Piasecki M. Light induced effects in chalcogenide glasses, glass-ceramics and crystals. Trans Indian Ceram Soc 2012;71:211–4.
[17] Simunek A, Vackar J. Hardness of covalent and ionic crystals: first principle calculations. Phys Rev Lett 2006, 96085501-1-085501-4.
[18] Li K, Wang X, Jhang F, Xue D. Electronegativity identification of novel superhard materials. Phys Rev Lett 2008;100, 235504-1-235504-4.
[19] Arora SK, Rao GST, Batra NM. Vickers micromechanical indentation of $BaMoO_4$ crystals. J Mater Sci 1984;19:297–302.
[20] Ghoneim NA, Batal HA, Nassar AMA. Microhardness and softening point of some alumino-borate glasses as flow dependent properties. J Non-Cryst Solids 1983;55:343–51.
[21] Miyata N, Jinno H. Fracture toughness and fracture surface energy of lead borate glasses. J Mater Sci Lett 1982;115:6–158.
[22] Savova E, Skordeva E, Vateva E. The topological phase transition in some Ge-Sb-S glasses and thin films. J Phys Chem Solids 1994;55:575–8.
[23] Skordeva E, Arsova DD. A topological phase transition in ternary chalcogenide thin films. J Non-Cryst Solids 1995;192:665–8.
[24] Tichy L, Ticha H. On the chemical threshold in chalcogenide glasses. Mater Lett 1994;21:313–9.
[25] Dergal A, Rahmoun K, Gueguin Y, Sangleboeuf JC, Keryvin V. Influence of the laser on the mechanical properties of $GeSe_9$ chalcogenide glasses. Phys Proc 2014;55:227–30.
[26] Kovanda V, Vlcek Mir, Jain H. Structure of As-Se and As-P-Se glasses studied by Raman spectroscopy. J Non-Cryst Solids 2003;326–327:88–92.